Single Cell Motion in Aggregates of Embryonic Cells

José C. M. Mombach* and James A. Glazier†

Department of Physics, University of Notre Dame, Notre Dame, Indiana 46556
(Received 8 September 1995)

We investigate the motion of individual pigmented retinal cells in aggregates of neural retinal cells obtained from chicken embryos. Individual cells in aggregates move randomly in the absence of chemical or adhesion gradients: the power spectrum of position and velocity versus time correspond to Brownian motion and the velocities are uncorrelated in time. Thus a quasithermal model of cell migration like the extended Potts model is appropriate. We also measure cell diffusivity and the cell velocity distribution. The results support the idea that collections of embryonic cells behave as liquids with membrane fluctuations playing the role of temperature.

PACS numbers: 87.45.Bp, 05.60.+w, 68.10.Cr

Some simple animals, such as sponges, sea urchins, or *Hydra,* can regenerate from a mixture of their dissociated cells. In more complex organisms, complete, whole body regeneration does not occur in adults. However, if individual organs from an embryo are dissociated into cells, which are then mixed and reaggregated, the cells sort and the resulting structure is very similar to the original one [1]. This sorting of biological cells to generate *homotypic* (like cell) cell domains has many similarities to the separation of mixtures of immiscible liquids. Recently, an experiment showed that the surface tension in aggregates of embryonic liver and heart cells of chicken embryos has area-invariant properties characteristic of liquid behavior [2].

The liquidlike behavior of collections of cells during cell sorting is important to the understanding of animal morphogenesis and is an open problem in physics.

Steinberg proposed an energy minimization theory, the differential adhesion hypothesis (DAH), to explain cell sorting [3]. In his theory, adhesion energies are associated with *homotypic* or *heterotypic* (unlike cell) interfaces and cell-medium interfaces and the minimization of the overall interface energy drives the evolution of the aggregate [3]. However, the DAH says nothing about the dynamics or mechanisms of the minimization.

In a previous paper we [4] found good quantitative agreement between a cell-sorting experiment and a model that includes differential adhesivity, the extended large-Q Potts model [5]. We found that the texture of the energy surface of cell sorting is rugged and that cell membrane fluctuations are necessary to drive the aggregate to its energy minimum, while avoiding trapping in metastable states. Now that the extended Potts model is being applied to more complex organisms [6], it is crucial to understand the limits of its biological realism.

The model is defined on a lattice by defining a spin, $\sigma(i,j)$, at each lattice site, (i,j). A given cell, σ, is defined by the set of all sites with the same spin. Each cell has an associated cell type, $\tau(\sigma)$. The energy per unit surface area depends on cell type, $E(\tau, \tau')$. The cell size is included as a target volume, $V(\tau)$, with membrane elasticity one. Thus, the total energy is

$$H = \sum_{i,j} \sum_{i'j'} E(\tau(\sigma), \tau(\sigma'))(1 - \delta_{\sigma,\sigma'})$$
$$+ \lambda \sum_{\sigma} [V(\tau(\sigma)) - \upsilon(\sigma)]^2, \qquad (1)$$

where $\upsilon(\sigma)$ is the volume of cell σ. We use a cubic lattice of $100 \times 100 \times 100$ sites where the initial state is a spheric aggregate surrounded by medium. The typical cell volume is about 100 sites. Values for simulation temperature, T, membrane elasticity, λ, and energies are discussed in [4]. We carry out the evolution using standard Monte Carlo and Boltzmann dynamics. In the model, when T increases, cell boundaries fluctuate with greater amplitude, simulating membrane fluctuations of real cells which should not be confused with the much smaller amplitude fluctuations due to thermal energy in experiments [4,5]. Increased membrane rigidity or contact energies are equivalent to reductions in the simulation temperature. In experiments the temperature is held at 37 °C, eliminating temperature dependent changes in membrane rigidity. These can be accommodated by changing the membrane elasticity in the model.

While the simulation, in general, requires five energies to specify cell-cell and cell-medium interactions, in our simple case of isolated cells only two interaction energies occur, pigmented-neural (d, l) and neural-neural (l, l). The relative size of these two energies will not qualitatively affect diffusion, which involves symmetrical creation and destruction of heterotypic interface at the expense of homotypic. Thus, our results should apply when $E(d, l) < E(l, l)$ (mixing) as well as for normal cell sorting.

Cell locomotion occurs through cytoskeletally driven contractions and expansions of the cell membrane. Adding cytochalasin B to the culture medium blocks cytoskeletal activity, stopping locomotion. We found that the presence of cytochalasin B in the culture medium yields results equivalent to those obtained from the extended Potts model simulation at low fluctuation temperatures. Additionally, when we transferred aggregates from medium containing

cytochalasin B into a culture medium free of the drug, the cell membrane activity recovered and the aggregates sorted normally. Holding the cells at 4 °C caused similar reversible inhibition of membrane fluctuations resulting in a temporary blocking of cell sorting. We concluded that membrane fluctuations in aggregates of biological cells play a role analogous to temperature in ordinary thermodynamics.

However, we were not able to verify that the fluctuation spectrum for real cells was the same as the spectrum for fluctuations in the model. Different fluctuation spectra might lead to substantially different rates of sorting and nonthermodynamic behaviors in the biological aggregates. In particular, the spectrum of the fluctuations affects the rate at which the configuration space diffuses in its energy landscape, where the rate of diffusion depends on the relation between the spectrum of cell and energy fluctuations. Physiologically, the fluctuation spectrum affects the rate of cell migration and the final completeness of cell sorting. We therefore must establish the validity of our thermodynamic model.

Recent results, identifying in *biological liquids* properties analogous to ordinary liquids, including surface tension and viscosity, stimulated an investigation of the motion of individual cells in aggregates to verify the analogy between the motion of biological cells in aggregates and the motion of molecules in liquids [2]. In this Letter we study the motion of individual pigmented retinal cells in aggregates of neural retinal cells to obtain the power spectrum, the diffusion constant, and the velocity distribution to compare to results for random walks and Potts model simulations.

In our experiments we used neural retinal and pigmented retinal cells obtained from eight-day old chick embryos and dissociated them using standard techniques (see Ref. [7]). To eliminate possible bias to the cell motion due to long range diffusible chemotactic agents which could be released by either cell type, we used a random mixture of neural retinal cells with either a single or a few very widely spaced pigmented retinal cells per aggregate, in a ratio of about 10^4 neural retinal cells to each pigmented retinal cell. Cells aggregated in a water bath with a gyratory shaker set to a speed of 80 rpm. After 24 h we selected an aggregate and transferred it to a 50 ml culture flask maintained at 37 °C on an inverted microscope for image recording. While it is possible to determine the full three dimensional trajectory of a cell [8,9], the spectra for random walks in two and three dimensions are the same. Thus to reduce the effort of data collection we performed two dimensional analyses only. We recorded the two dimensional motion (actually, a projection of the three dimensional motion) of a set of five pigmented retinal cells randomly chosen in the aggregate for 30 h at intervals of 30 min or more. Because the pigmented cells are at least several cell diameters away from the boundaries of the neural retinal cell clusters, and since gravitational

effects, if present, are extremely weak, we expect that motion in the vertical direction will be indistinguishable from motion in the horizontal, an observation borne out by the undistorted spherical symmetry of fully sorted cell clusters. The time interval was chosen by comparing the average displacement of the cells and the cell diameter. In 30 min a pigmented retinal displaces a small fraction ($\sim 1/6$) of its diameter. We present a plot of the motion of the cells with their initial and final positions in Fig. 1.

The observed cell aggregate gradually changed its shape to minimize its surface according to the DAH. This rounding dragged the observed set of cells to different positions even though the position of the culture flask containing the aggregate on the stage microscope was fixed. However, we wished to study the motion of cells with respect to the aggregate, not bulk aggregate motion. In order to approximate reference points fixed in relation to the aggregate, we chose two independent references: the center of mass of the set, CMS (supposing pigmented cells of equal masses), and the position of the least moving cell, LMCS (cell indicated by an asterisk in Fig. 1). Neither reference system is strictly steady in relation to the cells, which introduces a small error in our measurements, but we stress that our main aim here is to report the nature of the cell motion and its consequences for the macroscopic behavior of cell aggregates.

Figure 1 shows the positions of the centers of the cells at different times in the CMS. The average diameter of the observed cells is about 8 μm. We can see from the figure that some cells moved much more than one cell diameter from their original positions after 30 h. We show the averaged power spectrum of position versus time for each coordinate for all cells in Fig. 2. The slopes of the linear fits to the spectra are 1.7 ± 0.1 for the LMCS and 1.8 ± 0.1 for the CMS both over $1\frac{1}{2}$ decades. We also calculated the power spectrum for the extended Potts
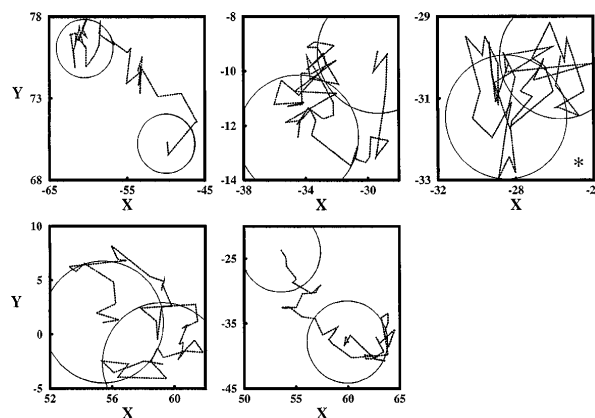

FIG. 1. Graph showing the initial and final positions occupied by the cells during the experiment in the center of mass reference frame (CMS set to zero). Circles represent the approximate size of the cells and the least moving cell is indicated by an asterisk. The scale is in μm.
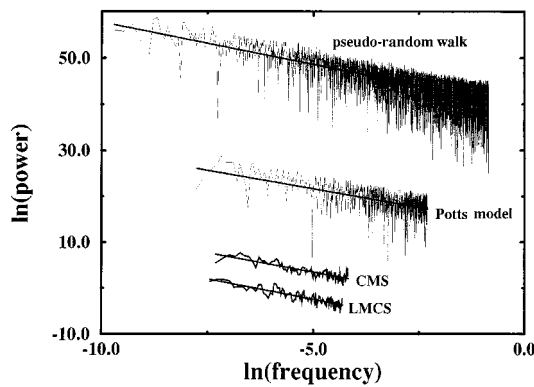
FIG. 2. Power spectra of position vs time for the cells in each reference system, the discrete pseudorandom walk, and Potts model simulation. The curves are offset vertically for easy visualization.

model simulation of a single dark cell in a light aggregate, obtaining 1.6 ± 0.07. For a simulation of a discrete pseudorandom walk with 2^{14} steps we obtained a slope of 1.82 ± 0.01, close to the expected scaling exponent of 2.0 for an infinite walk. Because the projection of a random walk is also a random walk, the result confirms our decision to neglect the third dimension in our calculations. Because of the small distances traveled over shorter times, the error in calculating the scaling is larger at higher frequencies. Preliminary measurements using a time interval of 2 min yield a slope of 1.4 ± 0.1, as expected due to zero slope measurement errors. We are currently conducting more precise measurements of this short term fluctuation.

We determined the temporal autocorrelation of the velocity for both experiment and theory (not shown). In both cases we obtained a single narrow peak at a lag of 0, reasonably approximating a *delta* function. The correlation time for the velocity was shorter than the measurement interval for both experiment (30 min) and simulation (5 MCS), agreeing with the hypothesis of time-uncorrelated velocities in Brownian motion. Preliminary results on shorter time scales do not show correlations. However, we are continuing our experimental observations to search for weak correlations.

We measured the average diffusion constants in both experiment and simulation by determining the slope of the plot $\langle z^2 \rangle$ vs time according to the relation

$$\langle z^2 \rangle = 2Dt, \qquad (2)$$

where D is an effective diffusion constant, t time, and z is the displacement, here the average between x and y displacements for cells in each reference system. We found $D = 2.1 \pm 0.05$ $\mu m^2/h$ in the LMCS and $D = 1.8 \pm 0.03$ $\mu m^2/h$ in the CMS verifying that it is much smaller than in simple nonbiological fluids; for example, the diffusion constant of gases in liquids is typically about 360 $\mu m^2/h$. D is smaller in the CMS than it is in the LMCS due to the inclusion of the least moving cell

in its calculation. This diffusion constant is the actual experimental rate at which a pigmented cell explores its neural-retinal environment. These results also establish that chemotaxis does not bias the cells, which perform true random walks. However, uncorrelated noise will yield Eq. (1) even for a nonthermal velocity spectrum.

In Fig. 3 we present a histogram for the velocity distribution of the cells, obtained by summing the histograms of individual cells in each reference system. We fit them to the functions $F(V) = a_0 V \exp(a_1 V^2)$ and $F(V) = a_0 V^2 \exp(a_1 V^2)$ which correspond to the functional form of the Maxwell distribution for the velocity of random particles in a gas in two and three dimensions, respectively [10]. Both simulated and experimental distributions agree within counting error to the appropriate Maxwell distribution, though poor statistics results in larger errors for the experimental data.

The results presented here in association with the thermodynamic DAH theory establish statistical mechanics foundations for the observed liquid properties of aggregates of embryonic cells. In the absence of external biases, cells perform a simple Brownian walk. Aggregates round in the same way that a liquid drop rounds; cells perform a biased random walk guided by energy minimization in a manner identical to simple liquids. Spherical symmetry results from simple energy minimization. Thus, the use of simple statistical mechanics models even for fairly complex problems in embryogenesis is appropriate.

In aggregates where more than one cell type is present, the random motion allows cells to explore their neighborhood to find another cell of the same type, explaining why aggregates containing a very dissimilar ratio of neural retinal and pigmented retinal cells (about 30 neural retinal cells to one pigmented retinal cell) are able to sort [4].
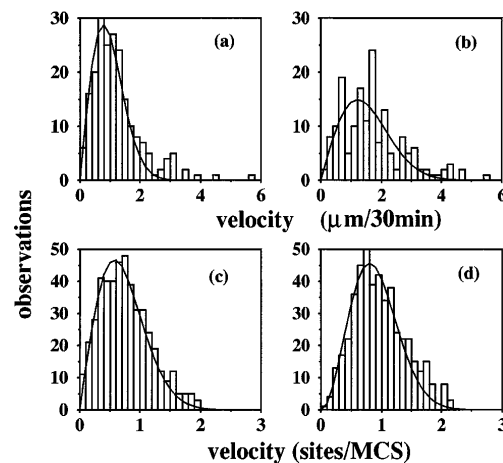

FIG. 3. Histogram of the two dimensional cell velocity distribution for (a) LMCS, (b) CMS, and (c) simulation. The solid curve is a fit by the function $F(V) = a_0 V \exp(a_1 V^2)$. (d) Plot of the three dimensional cell velocity distribution for the simulation. The solid curve is a fit by the function $F(V) = a_0 V^2 \exp(a_1 V^2)$.

In principle, arbitrarily dilute aggregates should eventually sort. However, if the time taken for cells to encounter each other by diffusion is very long, they will not have time to sort before other biological processes intervene and the sorting will remain partial.

Additionally, the data did not show a tendency of the cells to find each other over long distances and cluster which excludes chemotaxis due to long range signaling between pigmented cells via diffusible messengers as a major underlying process in this simple type of cell sorting.

We are currently investigating additional liquid properties of embryonic cells, including short term center of mass spectra, measurement of viscosities, and the power spectrum of the fluctuations of the cellular membrane. Our goal is to establish the degree to which a thermodynamic model of cell sorting is applicable and its consequences for morphogenesis.

---

*Permanenet address: Instituto de Física, Universidade Federal do Rio Grande do Sul, Caixa Postal 15051, 91501–970 Porto Alegre, RS, Brazil.
Electronic address: jose@if1.if.ufrgs.br
†Corresponding author.
Electronic address: jglazier@rameau.phys.nd.edu

[1] S. G. Lenhoff, *Hydra and the Birth of Experimental Biology – 1744* (The Boxwood Press, Pacific Grove, 1986); P. L. Townes and J. Holtfreter, J. Exp. Zool. **128**, 53 (1955); P. B. Armstrong, Crit. Rev. Biochem. Mol. Biol. **24**, 119–149 (1989); S. A. Newman and W. D. Comper, Development **110**, 1 (1990).

[2] R. A. Foty, G. Forgacs, C. M. Pfleger, and M. S. Steinberg, Phys. Rev. Lett. **72**, 2298 (1994).

[3] M. S. Steinberg, Science **141**, 401 (1963).

[4] J. C. M. Mombach, J. A. Glazier, R. C. Raphael, and M. Zajac, Phys. Rev. Lett. **75**, 2244 (1995).

[5] F. Graner and J. A. Glazier, Phys. Rev. Lett. **69**, 2013 (1992); J. A. Glazier and F. Graner, Phys. Rev. E **47**, 2128 (1993); J. A. Glazier, R. C. Raphael, F. Graner, and Y. Sawada, in *Proceedings of Interplay of Genetic and Physical Processes in the Development of Biological Form,* edited by D. Beysens, G. Forgacs, and F. Gaill (World Scientific, Singapore, 1995), p. 54.

[6] N. Saville and P. Hogeweg (unpublished).

[7] P. B. Armstrong and D. Parenti, J. Cell Biol. **55**, 606 (1972).

[8] C. Hug, P. Y. Jay, I. Reddy, J. G. McNally, P. C. Bridgman, E. L. Elson, and J. A. Cooper, Cell **81**, 591 (1995).

[9] K. W. Doolittle, I. Reddy, and J. G. McNally, Dev. Biol. **167**, 118 (1995).

[10] F. Reif, *Fundamentals of Statistical and Thermal Physics* (McGraw-Hill, Inc., New York, 1965).